Online Resource B (ESM_B.pdf): Supplementary Figures for Section 5

September 2023

by

Moritz Tarach

Technical University of Darmstadt, Department of Law and Economics
Hochschulstraße 1, D-64289 Darmstadt, Germany
e-mail: tarach@vwl.tu-darmstadt.de, tel.: +49 6151 1657 284

B Supplementary Figures for Section 5 of "Bottom-up Aggregation of Field-Level Oil Production Profiles via a Successive Sampling Discovery Model and a Birth Process: An Application to the Gulf of Mexico and Norway"

Figure B.1: Actual oil (black) and gas (red) production for the three regions

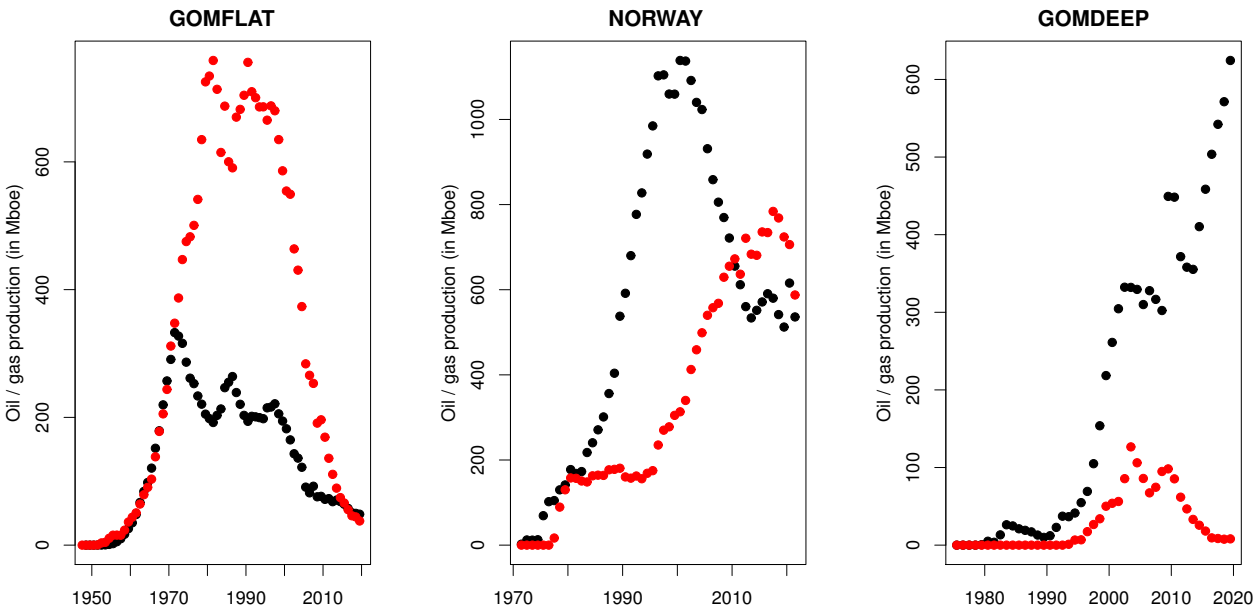

Figure B.2: Discovery and exploration history - GOM Flat

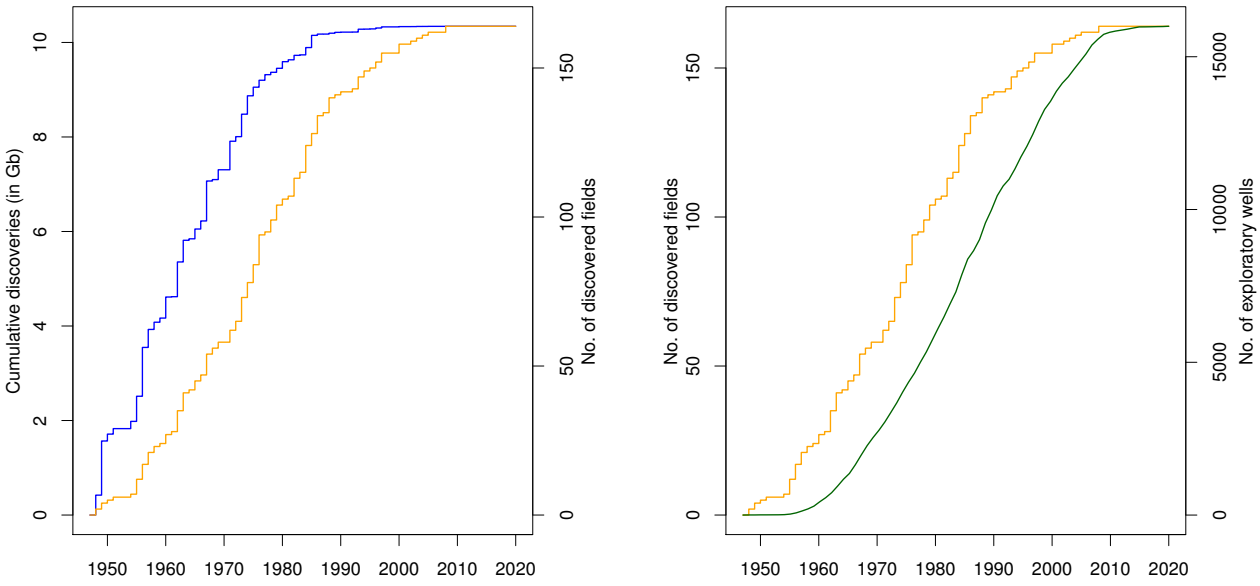

Note: depicted are the cumulative amounts of discovered oil (blue), the cumulative number of discovered oil fields (orange), and the cumulative number of drilled exploratory wells (green)

Figure B.3: Discovery and exploration history - Norway

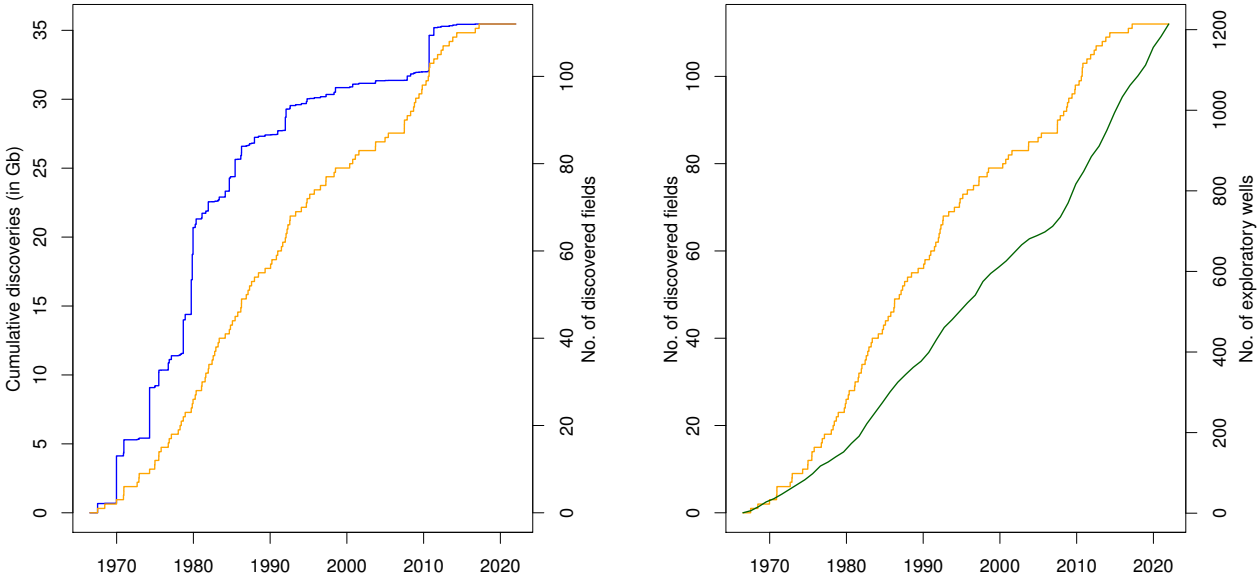

Note: depicted are the cumulative amounts of discovered oil (blue), the cumulative number of discovered oil fields (orange), and the cumulative number of drilled exploratory wells (green)

Figure B.4: Discovery and exploration history - GOM Deep

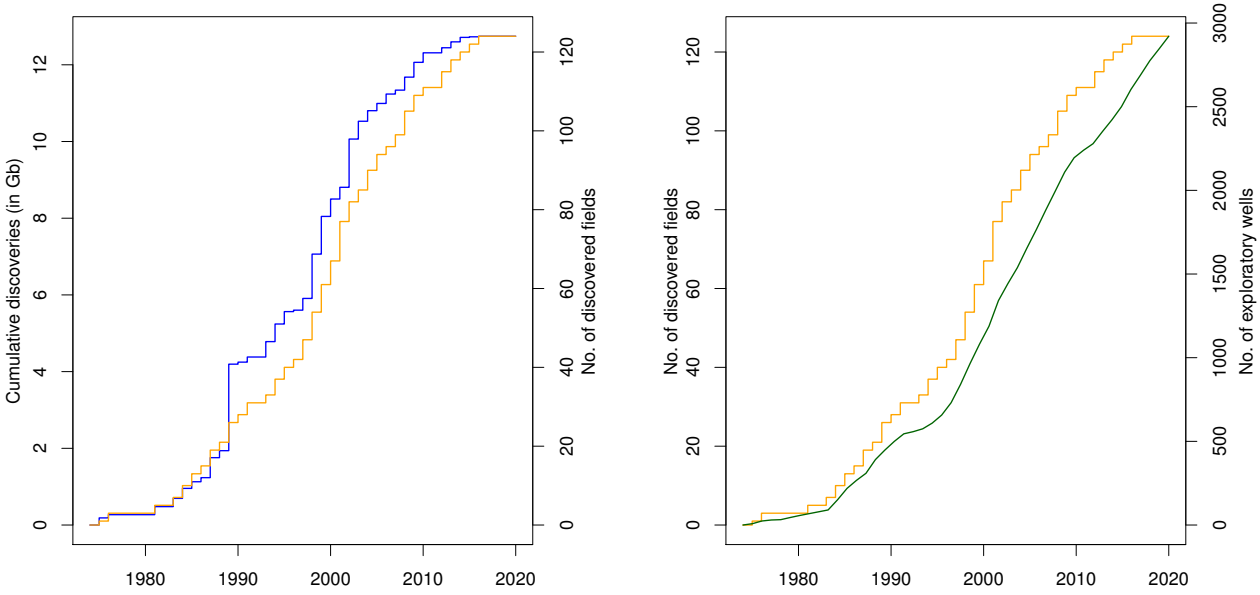

Note: depicted are the cumulative amounts of discovered oil (blue), the cumulative number of discovered oil fields (orange), and the cumulative number of drilled exploratory wells (green)

Figure B.5: Illustration of the depletion effect - GOM Flat

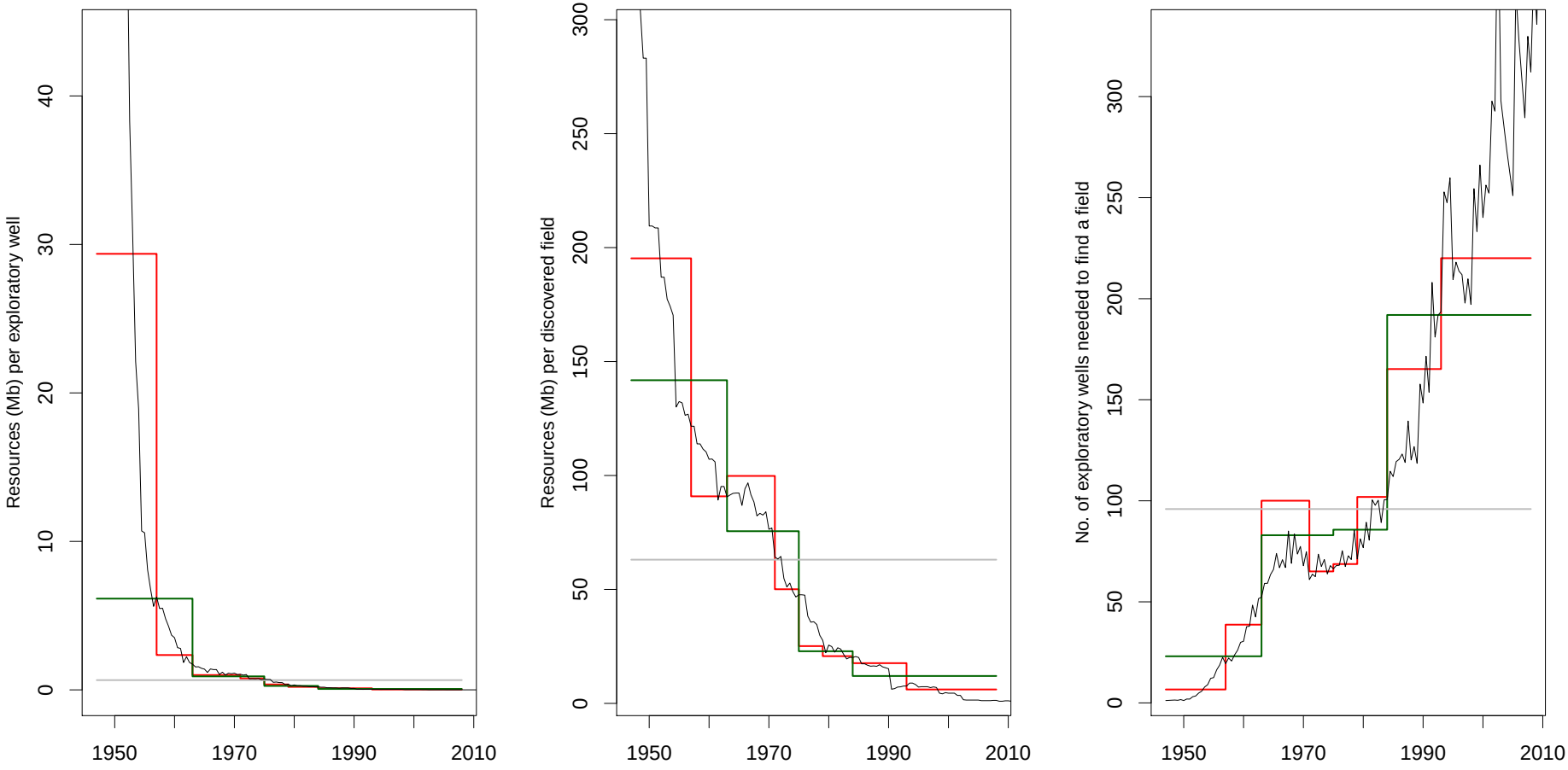

Note: the gray line depicts the average over all discovered fields, while for the green and the red lines the sample is divided into 4 and 8 equally-sized groups, respectively. The black line shows a moving average computed using a time-window of 10 years.

Figure B.6: Illustration of the depletion effect - Norway

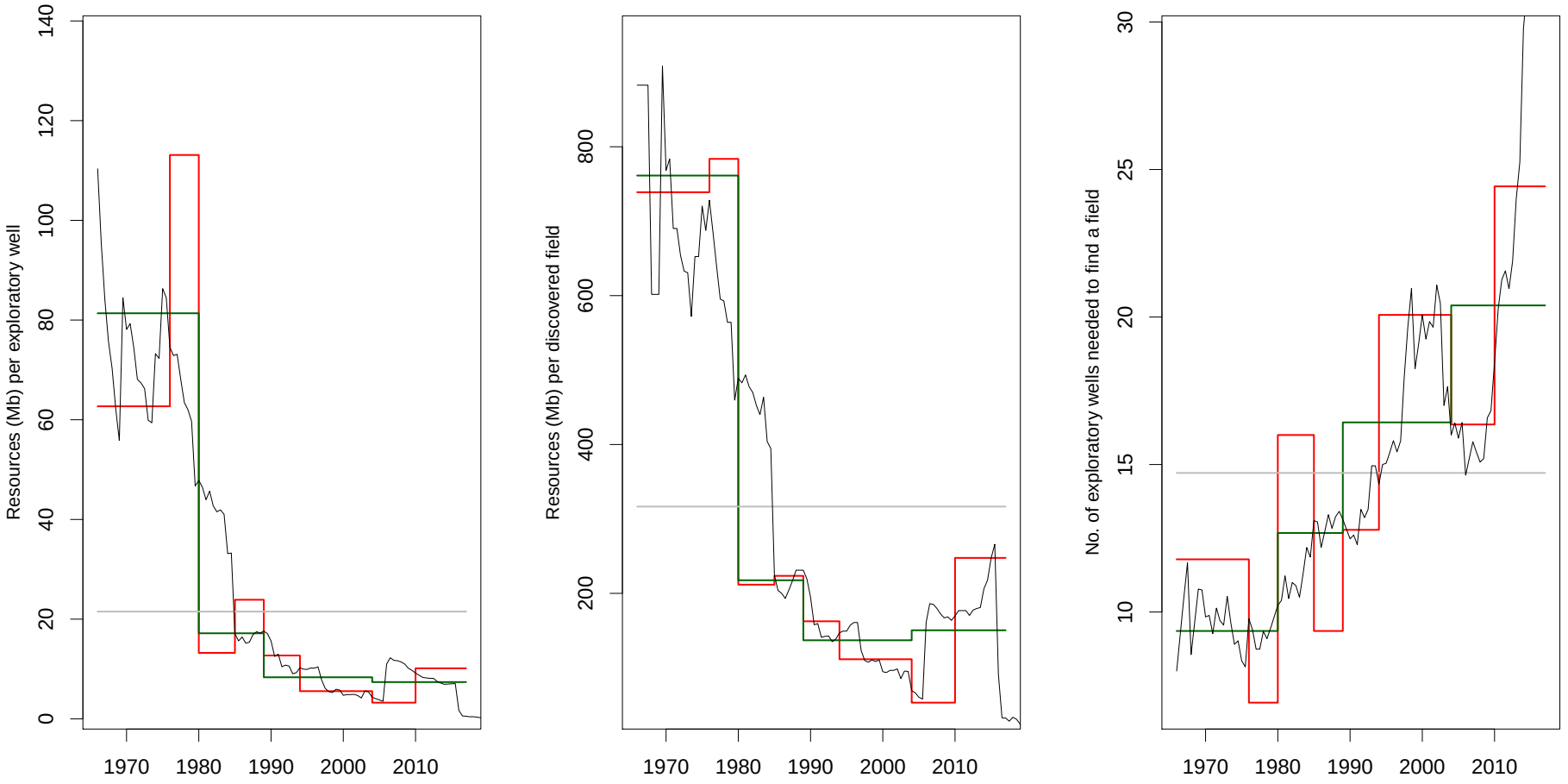

Note: the gray line depicts the average over all discovered fields, while for the green and the red lines the sample is divided into 4 and 8 equally-sized groups, respectively. The black line shows a moving average computed using a time-window of 10 years.

Figure B.7: Illustration of the depletion effect - GOM Deep

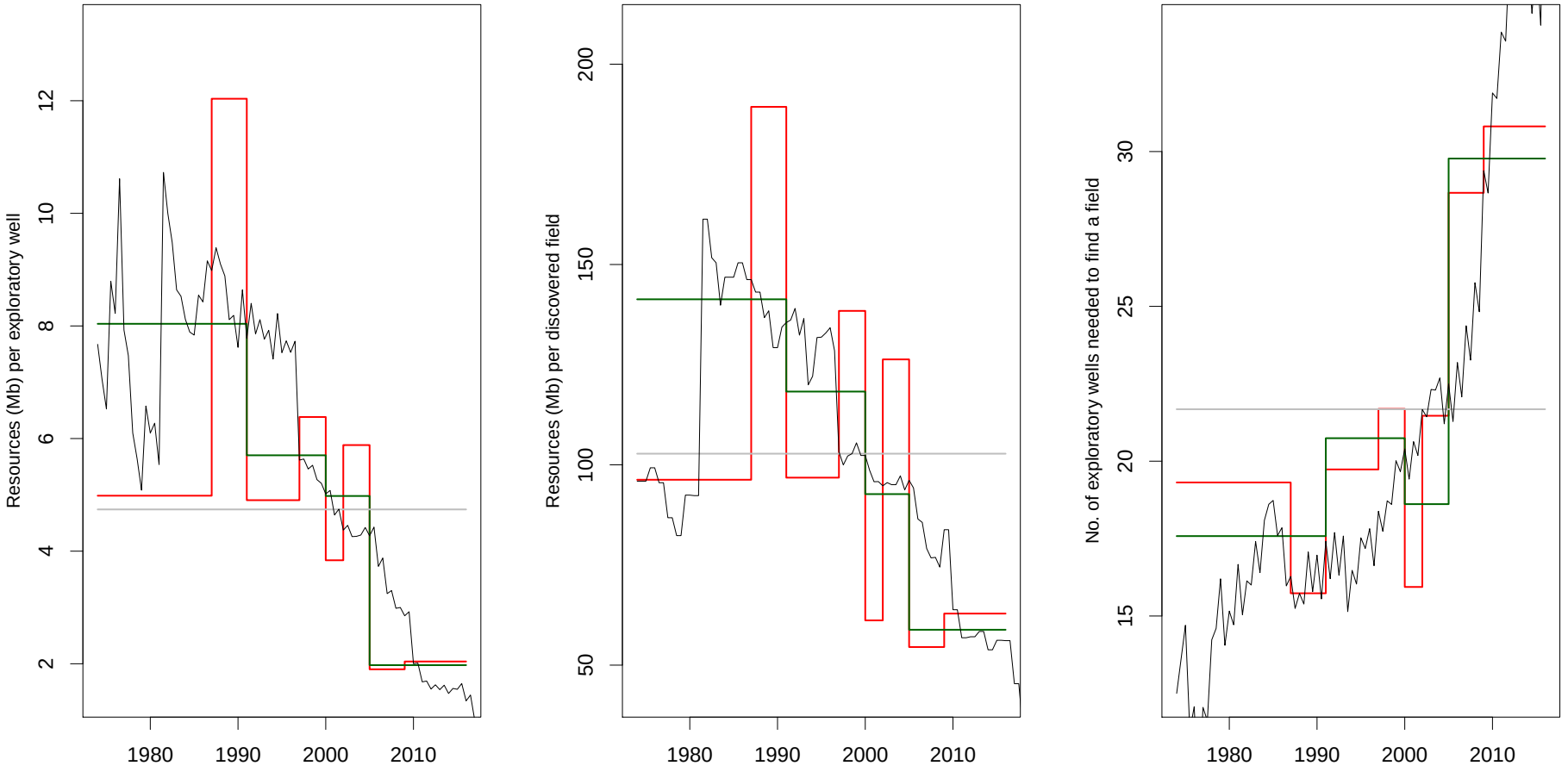

Note: the gray line depicts the average over all discovered fields, while for the green and the red lines the sample is divided into 4 and 8 equally-sized groups, respectively. The black line shows a moving average computed using a time-window of 10 years.

Table B.1: Estimation results for $\hat{a}_0$ and $\hat{b}_0$

	GOM Flat, $\underline{t} = 1962$		GOM Flat, $\underline{t} = 1967$		Norway, $\underline{t} = 1984$		Norway, $\underline{t} = 1989$	
$\overline{x}$	600	600	600	600	4400	4400	4400	4400
ν	164	164	164	164	150	150	150	150
	ML-EST	FIT-URR	ML-EST	FIT-URR	ML-EST	FIT-URR	ML-EST	FIT-URR
e_{k+1}	27308	8686	1772	812	628	311	526	221
$\hat{a}_0$	1.00	1.00	1.00	1.00	7.14	5.59	1.70	1.00
	(NA)[a]	(NA)	(NA)	(NA)	(1.82)	(3.72)	(1.91)	(NA)
$\frac{\hat{b}_0}{\hat{a}_0 e_{k+1}}$	19.69	17.20	45.22	32.50	0.27	0.62	7.71	11.93
	(6.29)	(5.82)	(4.06)	(3.26)	(0.36)	(1.14)	(10.20)	(1.09)
R^2	0.21	0.10	0.52	0.31	0.05	0.05	0.51	0.42

Note: HAC (Newey/West) standard errors are in parenthesis.
[a]Whenever $\hat{a}_0 < 1$ is obtained we set $\hat{a}_0 = 1$, hence no standard errors are available.

	Norway, $\underline{t} = 2022$		GOM Deep, $\underline{t} = 2000$		GOM Deep, $\underline{t} = 2005$		GOM Deep, $\underline{t} = 2020$	
$\overline{x}$	4400	4400	700	700	700	700	700	700
ν	150	150	300	300	300	300	300	300
	ML-EST	FIT-URR	ML-EST	FIT-URR	ML-EST	FIT-URR	ML-EST	FIT-URR
e_{k+1}	95	38	64	102	644	58	561	25
$\hat{a}_0$	3.97	1.00	1.00	1.00	3.88	1.77	1.96	1.00
	(3.05)	(NA)[a]	(NA)	(NA)	(4.97)	(5.96)	(2.08)	(NA)
$\frac{\hat{b}_0}{\hat{a}_0 e_{k+1}}$	7.26	29.27	12.36	12.15	2.88	7.54	10.81	22.11
	(8.08)	(3.80)	(1.12)	(1.12)	(5.22)	(29.34)	(13.06)	(1.00)
R^2	0.33	0.30	0.14	0.13	0.17	0.18	0.58	0.57

Note: HAC (Newey/West) standard errors are in parenthesis.
[a]Whenever $\hat{a}_0 < 1$ is obtained we set $\hat{a}_0 = 1$, hence no standard errors are available.

Figure B.8: Estimation results for GOM Flat ($\underline{t}$ =1962)

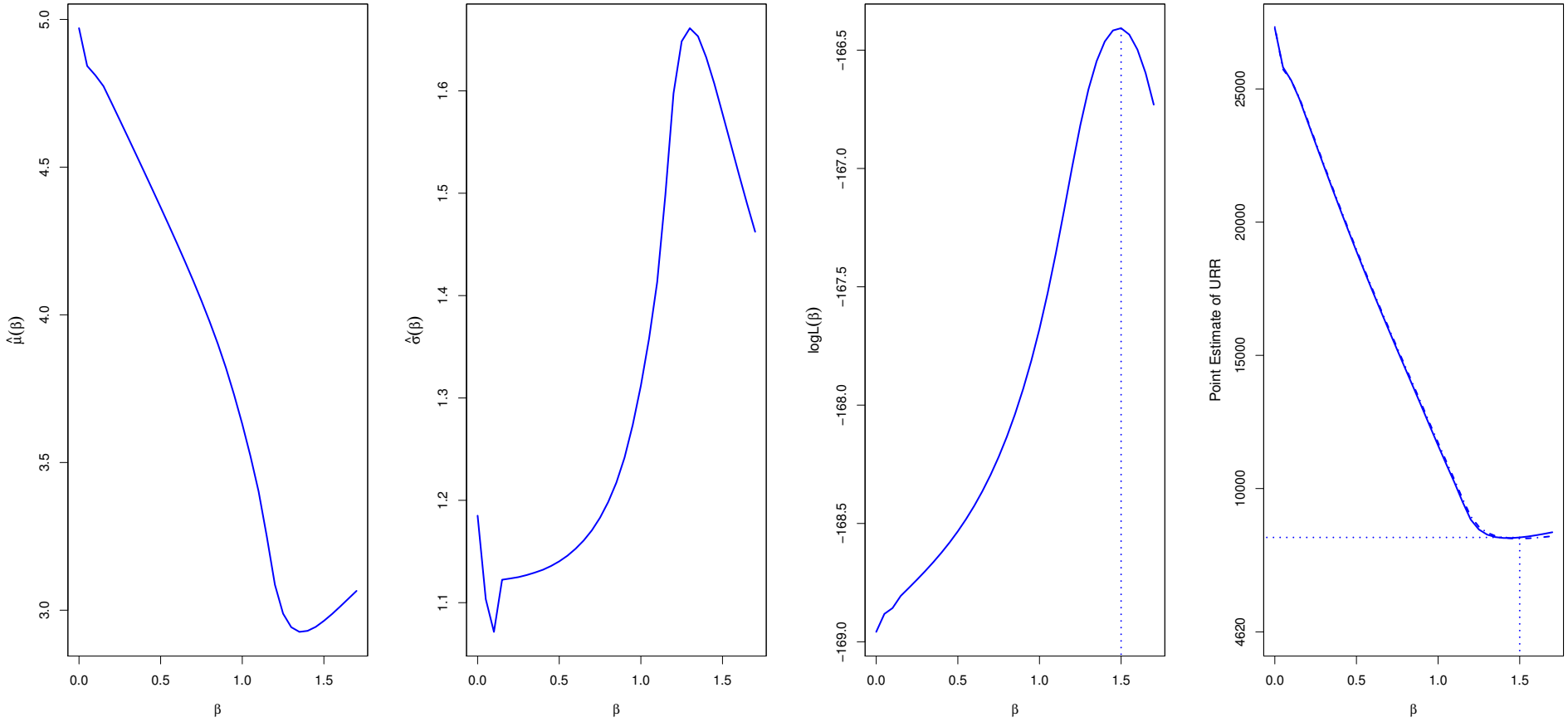

Note: the curves depict estimation results for $\nu = 164$. In the last panel the dot-dashed lines show the prior mean, while the solid lines show the posterior mean including the observed field sizes.

Figure B.9: Estimation results for GOM Flat ($\underline{t}$ =1967)

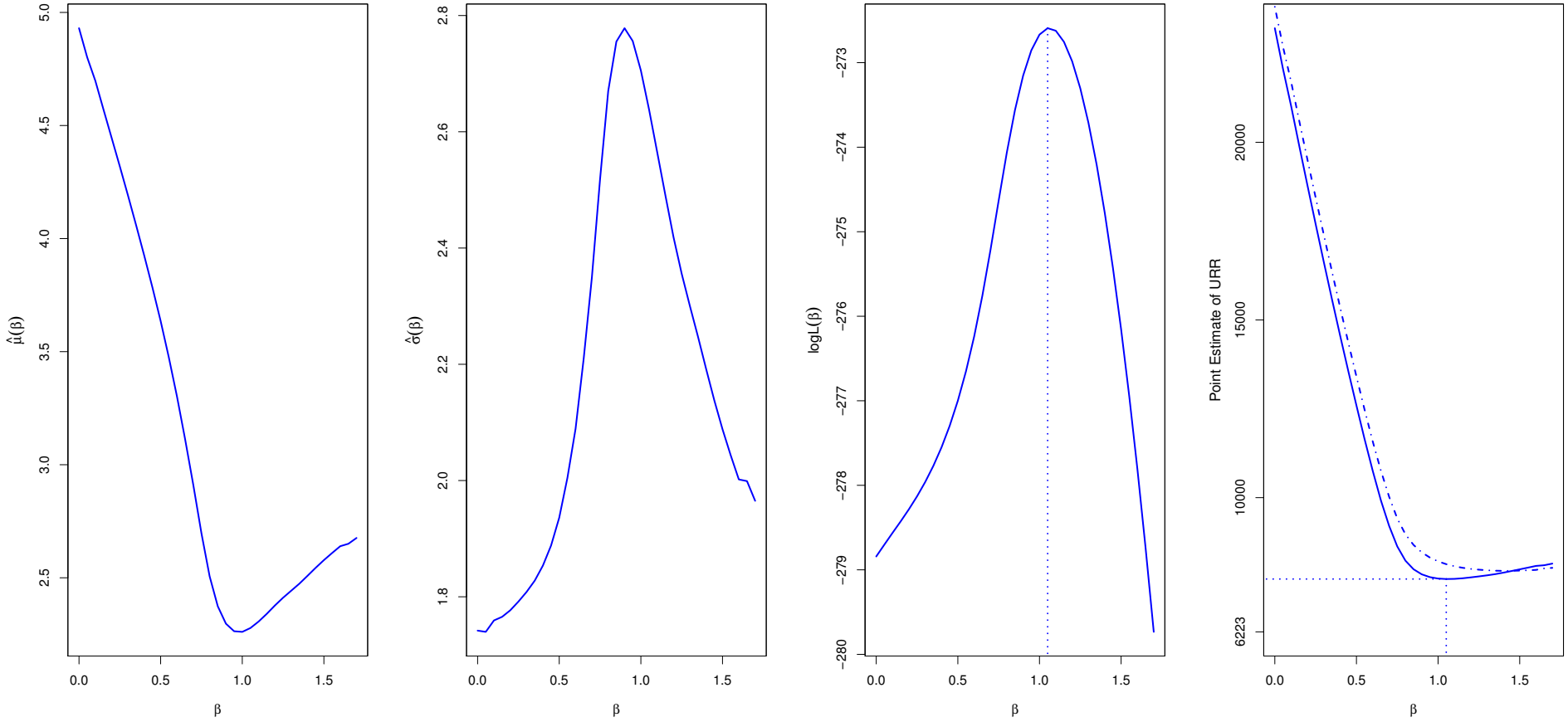

Note: the curves depict estimation results for $\nu = 164$. In the last panel the dot-dashed lines show the prior mean, while the solid lines show the posterior mean including the observed field sizes.

Figure B.10: Estimation results for Norway ($\underline{t}$ =1984)

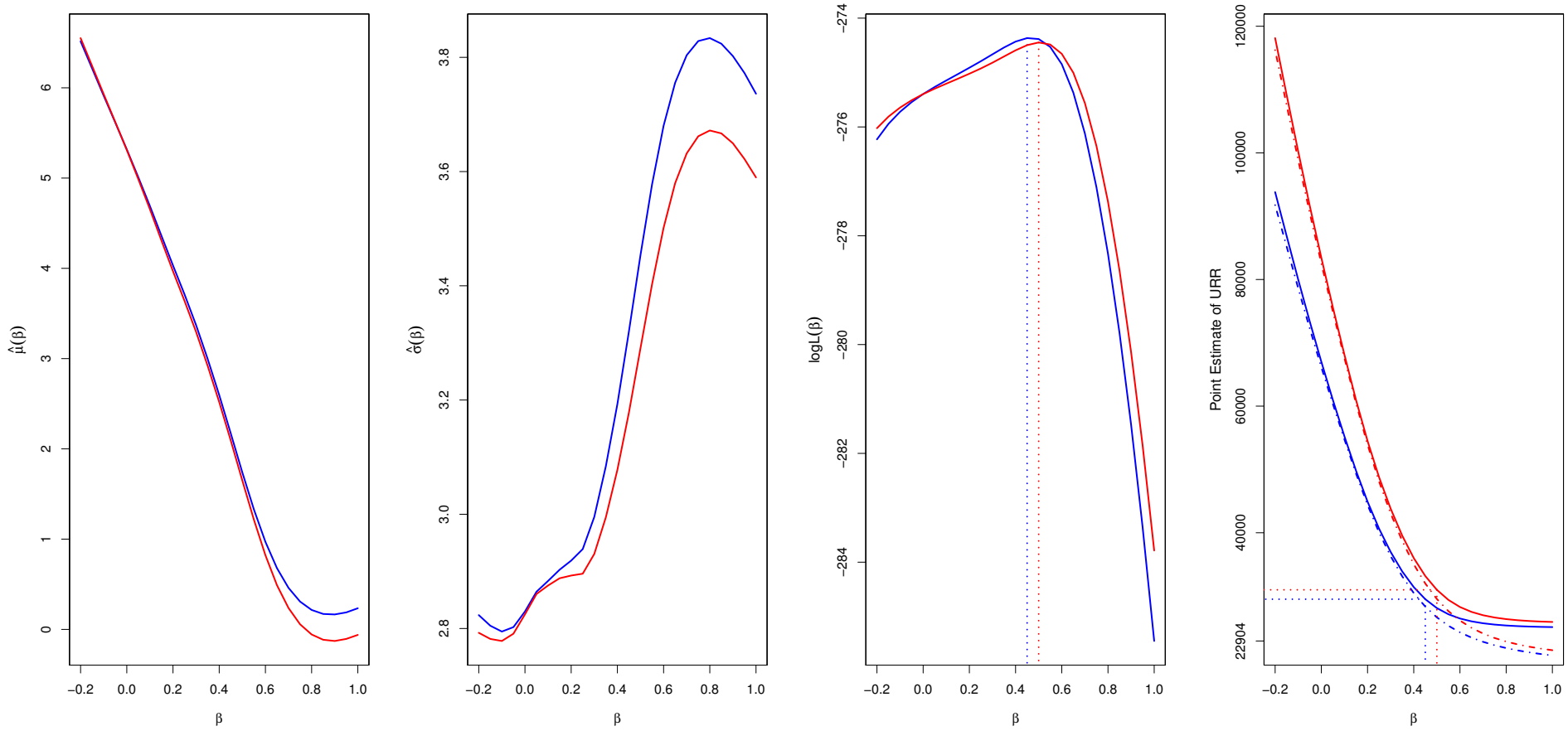

Note: the curves depict estimation results for $\nu = 150$ (in red) and $\nu = 120$ (in blue). In the last panel the dot-dashed lines show the prior mean, while the solid lines show the posterior mean including the observed field sizes.

Figure B.11: Estimation results for Norway ($\underline{t}$ =2022)

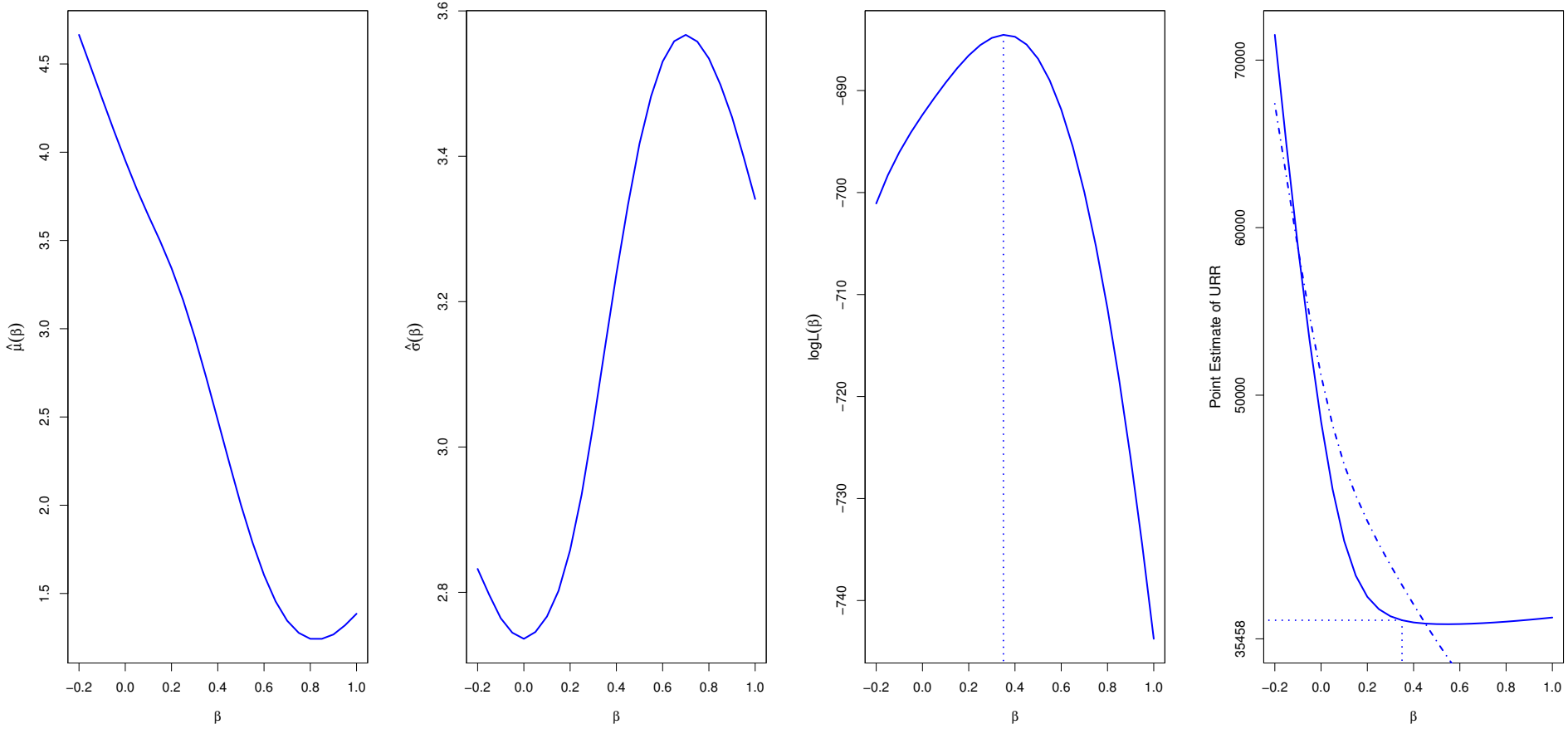

Note: the curves depict estimation results for $\nu = 150$. In the last panel the dot-dashed lines show the prior mean, while the solid lines show the posterior mean including the observed field sizes.

Figure B.12: Estimation results for GOM Deep ($\underline{t}$ =2000)

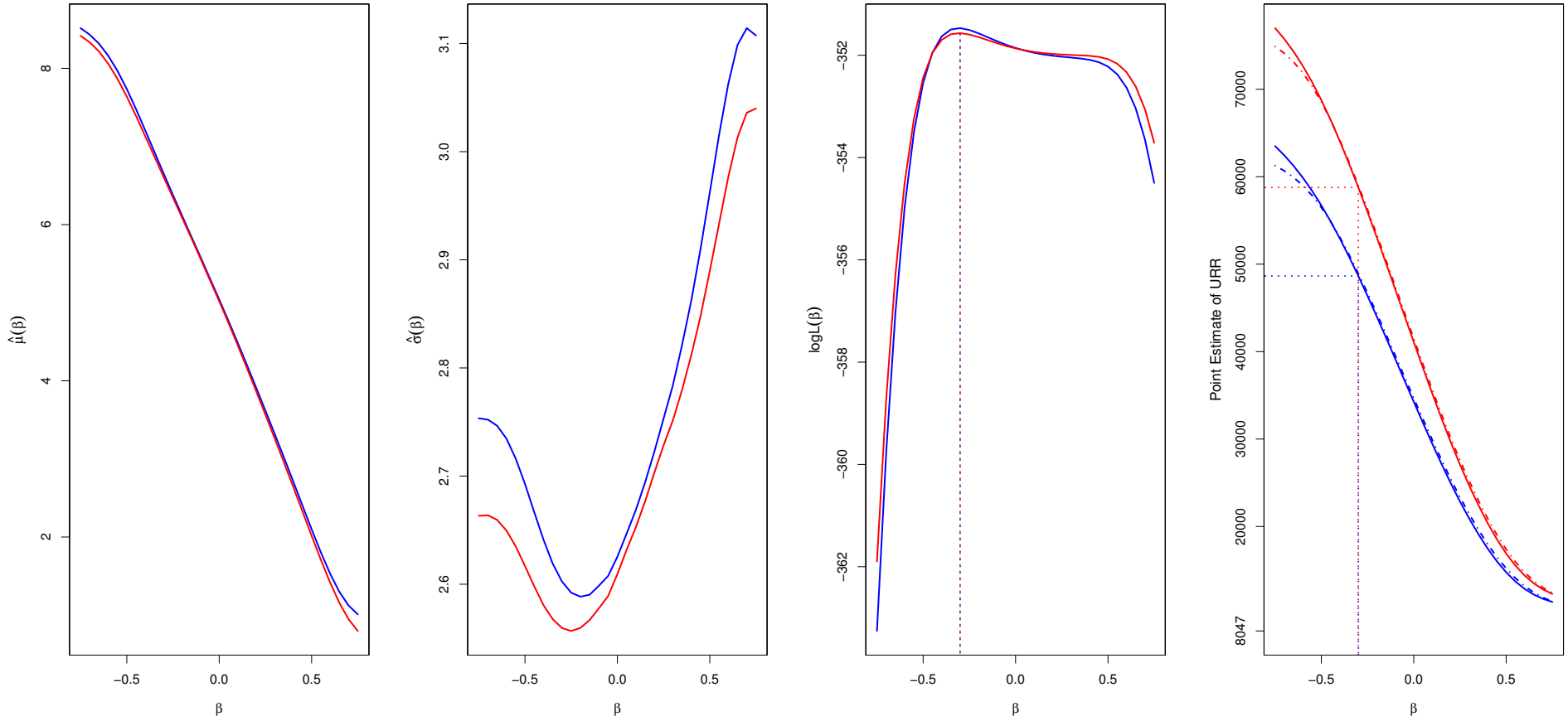

Note: the curves depict estimation results for $\nu = 300$ (in red) and $\nu = 250$ (in blue). In the last panel the dot-dashed lines show the prior mean, while the solid lines show the posterior mean including the observed field sizes.

Figure B.13: Estimation results for GOM Deep ($\underline{t}$ =2005)

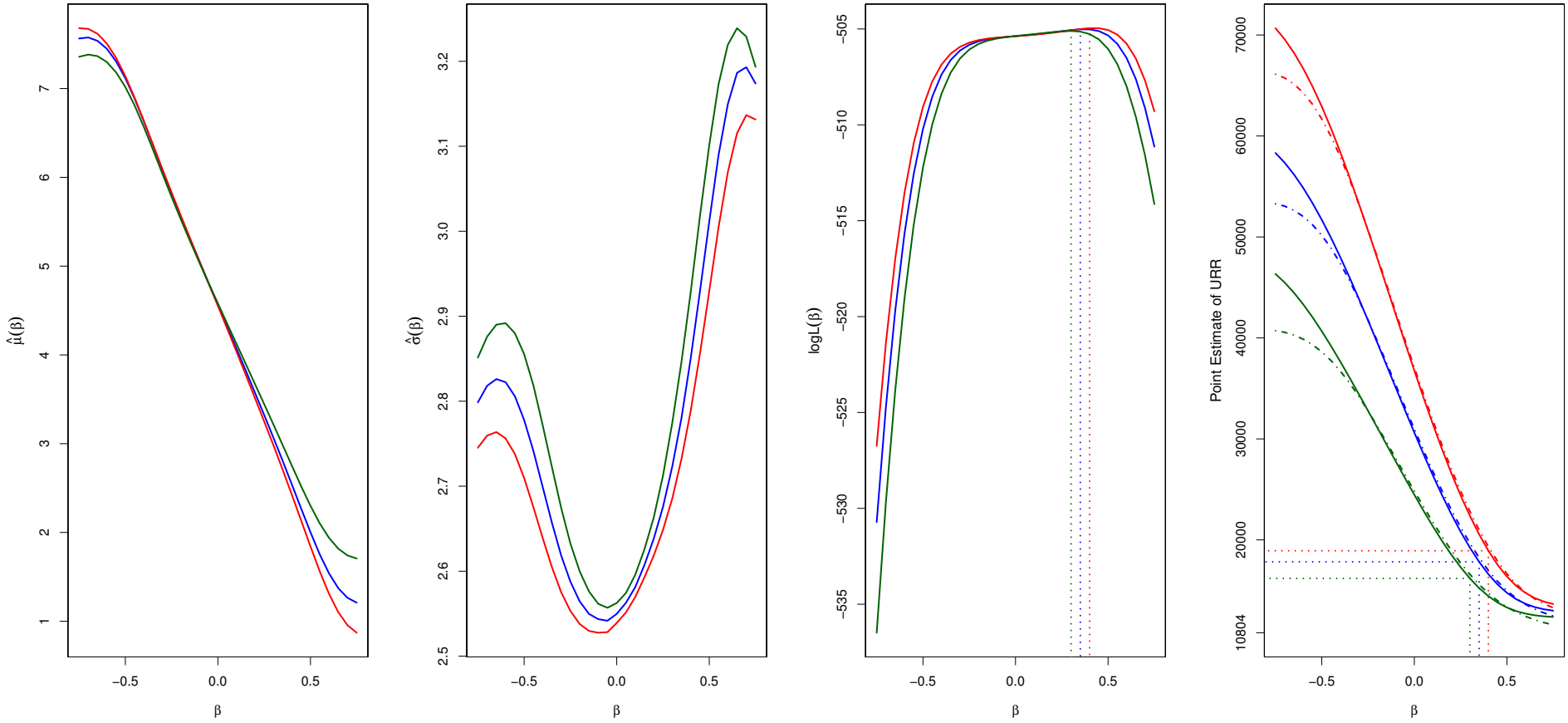

Note: the curves depict estimation results for $\nu = 300$ (in red), $\nu = 250$ (in blue), and $\nu = 200$ (in green). In the last panel the dot-dashed lines show the prior mean, while the solid lines show the posterior mean including the observed field sizes.

Figure B.14: Estimation results for GOM Deep ($\underline{t}$ =2020)

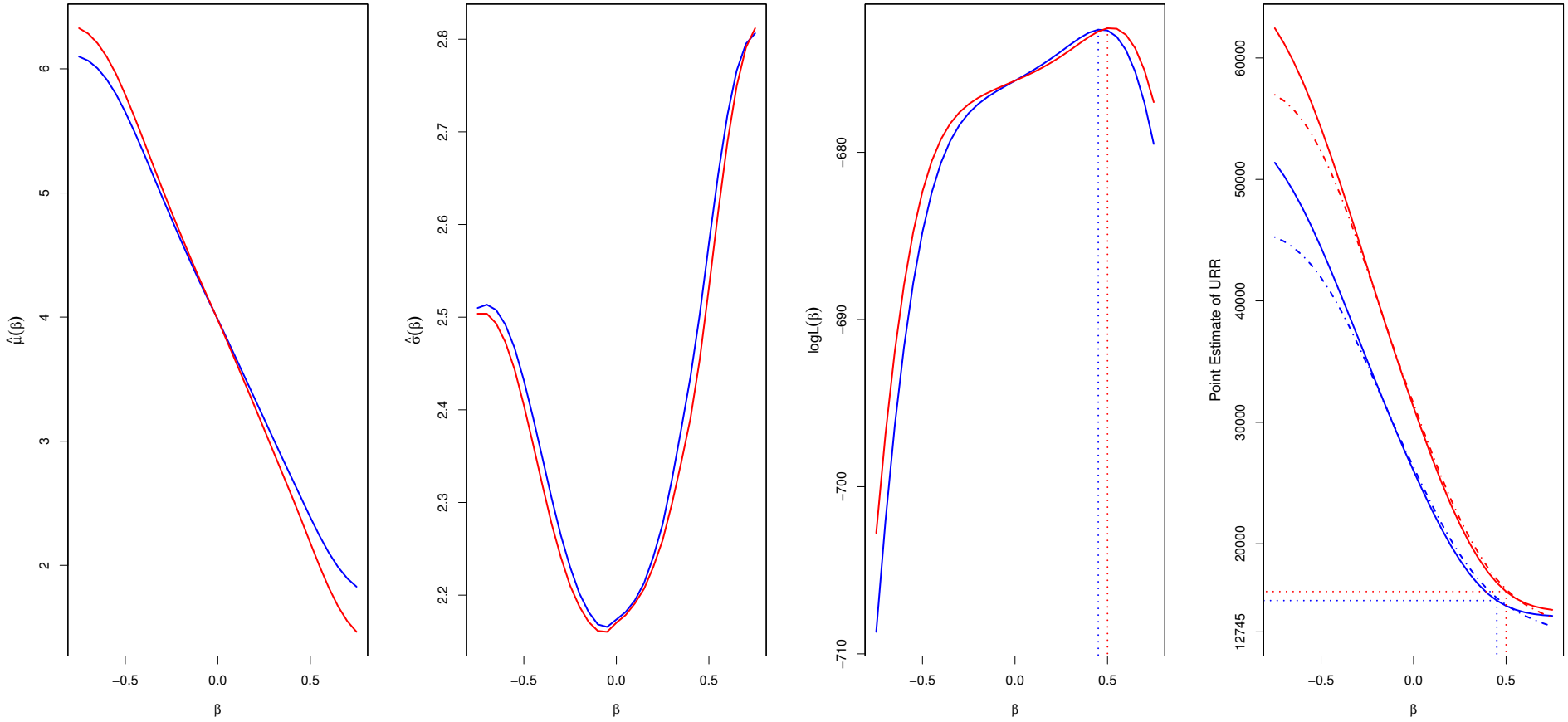

Note: the curves depict estimation results for $\nu = 300$ (in red), $\nu = 250$ (in blue). In the last panel the dot-dashed lines show the prior mean, while the solid lines show the posterior mean including the observed field sizes.

Figure B.15: Simulation results for GOM Flat ($\underline{t} = 1962$, FIT-URR, assumption (4b))

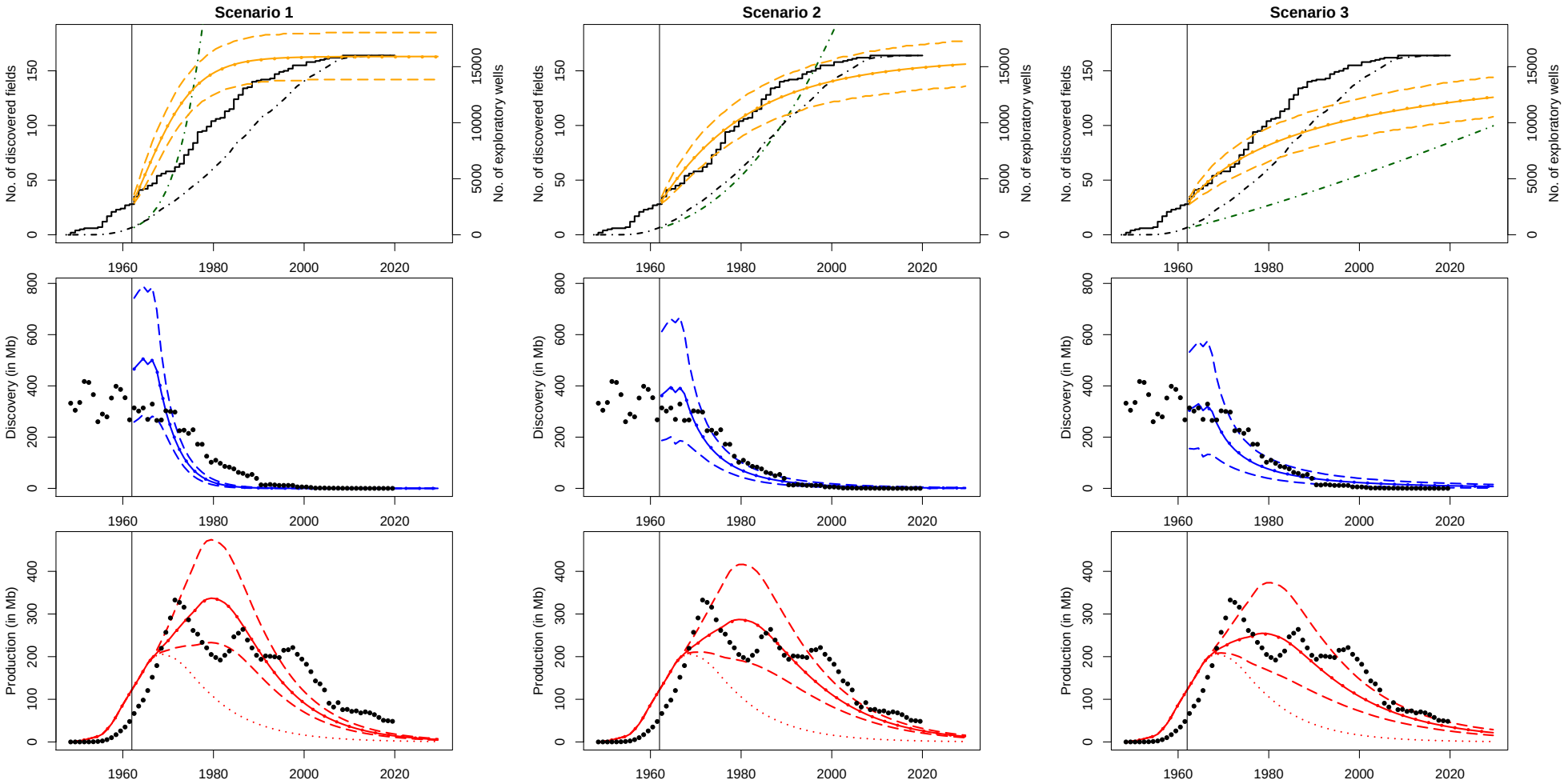

Figure B.16: Simulation results for GOM Flat ($\underline{t} = 1962$, FIT-URR, assumption (4a))

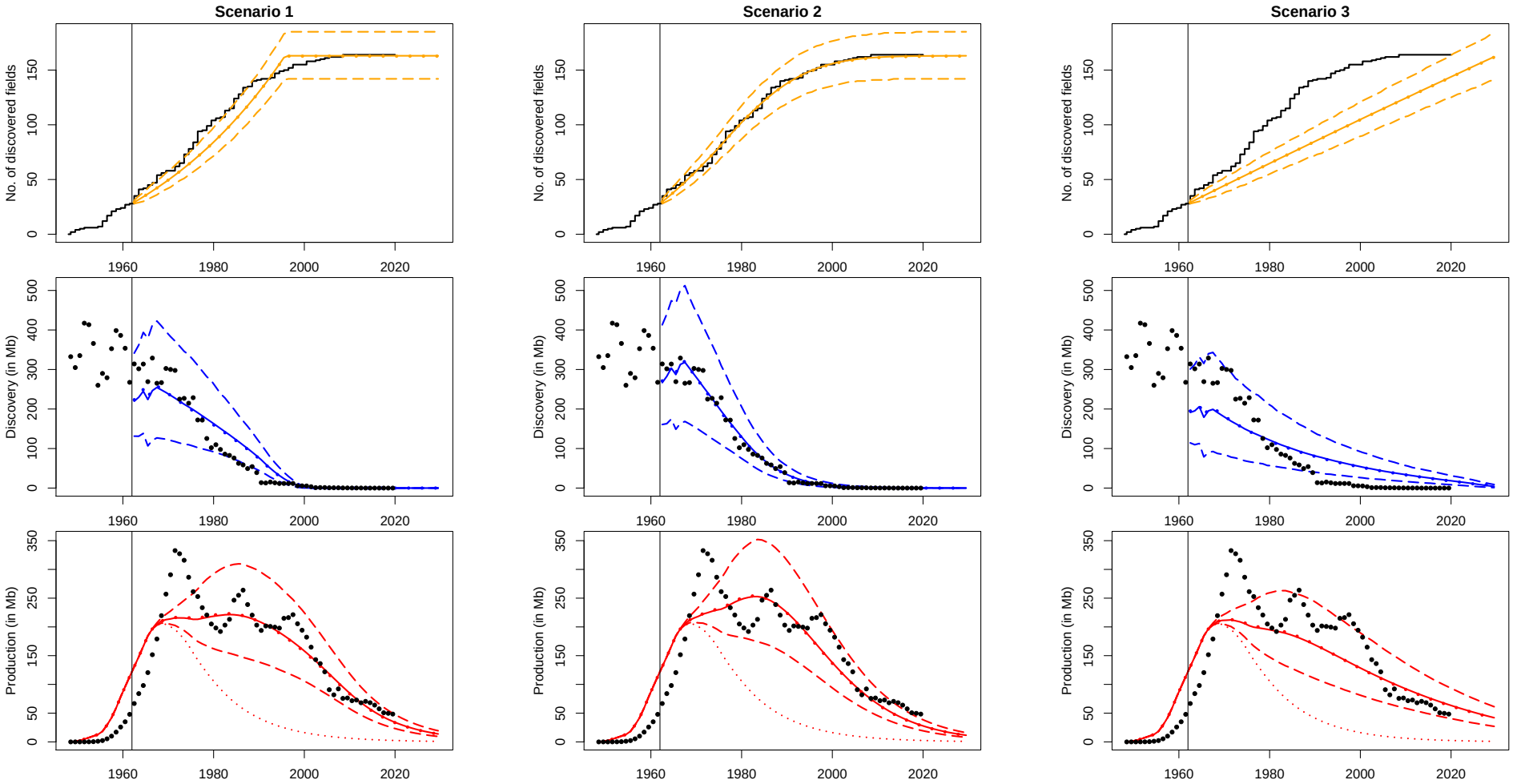

Figure B.17: Simulation results for Norway ($\underline{t} = 1984$, FIT-URR, assumption (4b))

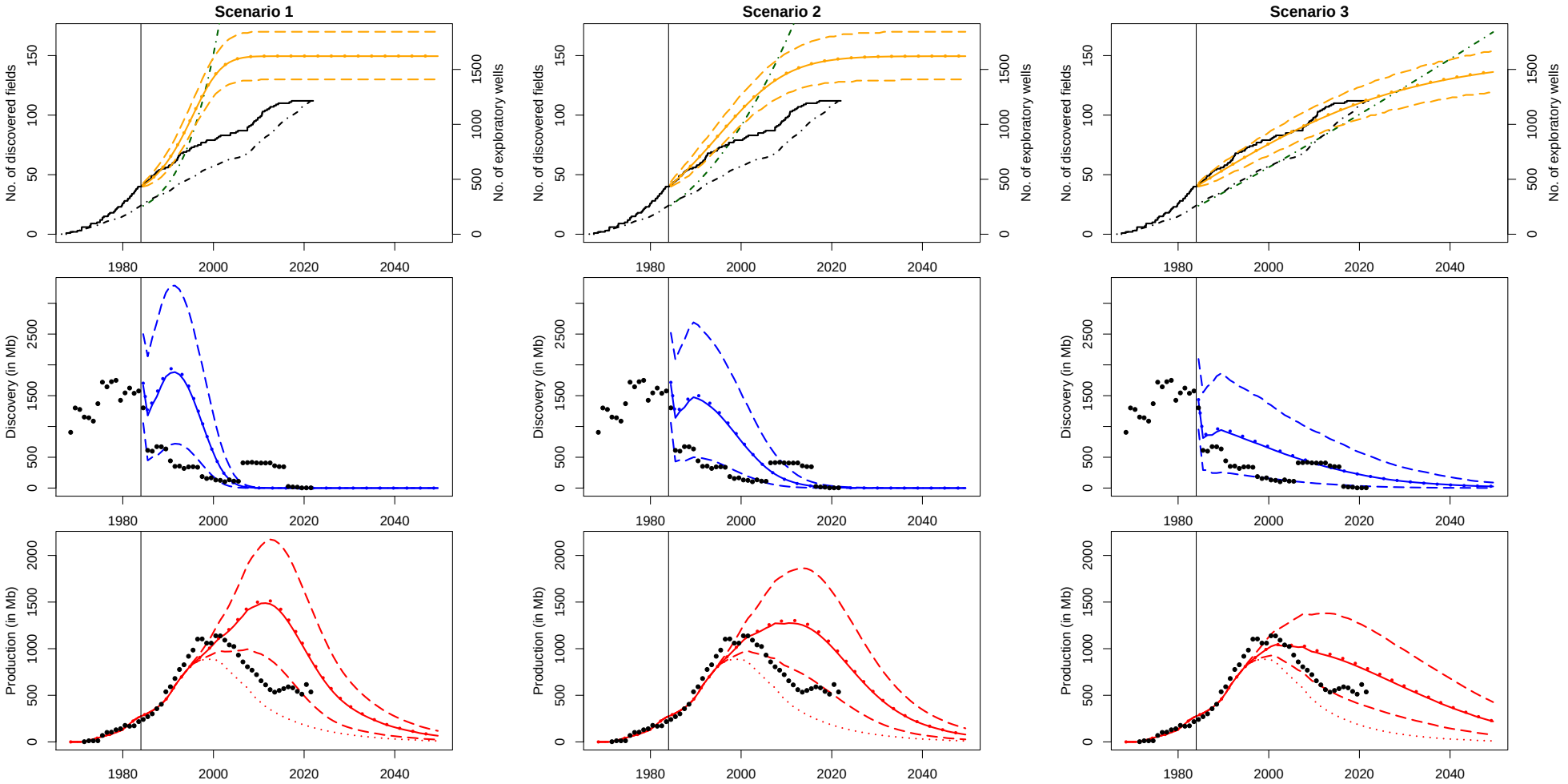

Figure B.18: Simulation results for Norway ($\underline{t} = 1984$, FIT-URR, assumption (4a))

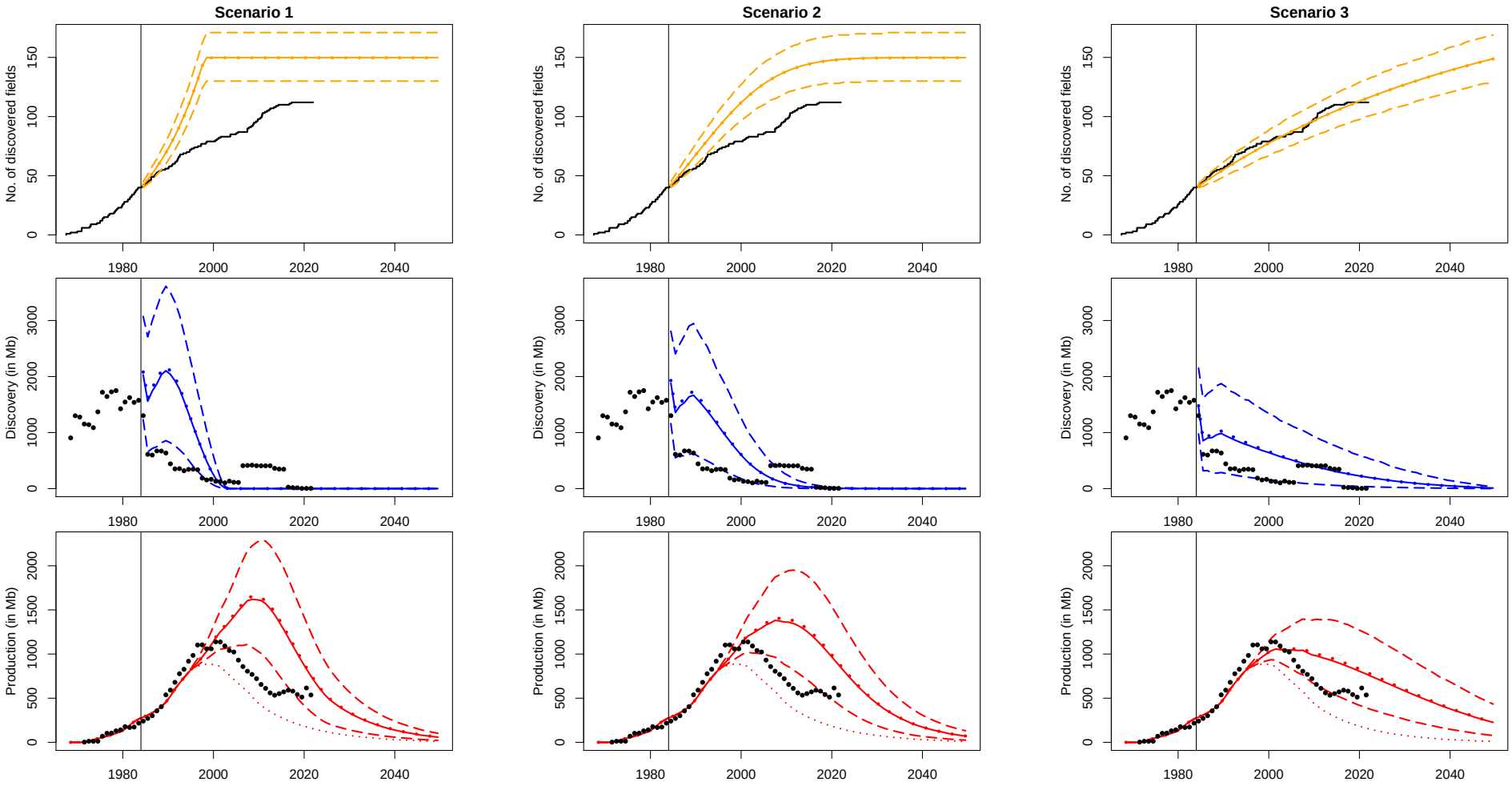

Figure B.19: Simulation results for Norway ($\underline{t} = 2022$, FIT-URR, assumption (4b))

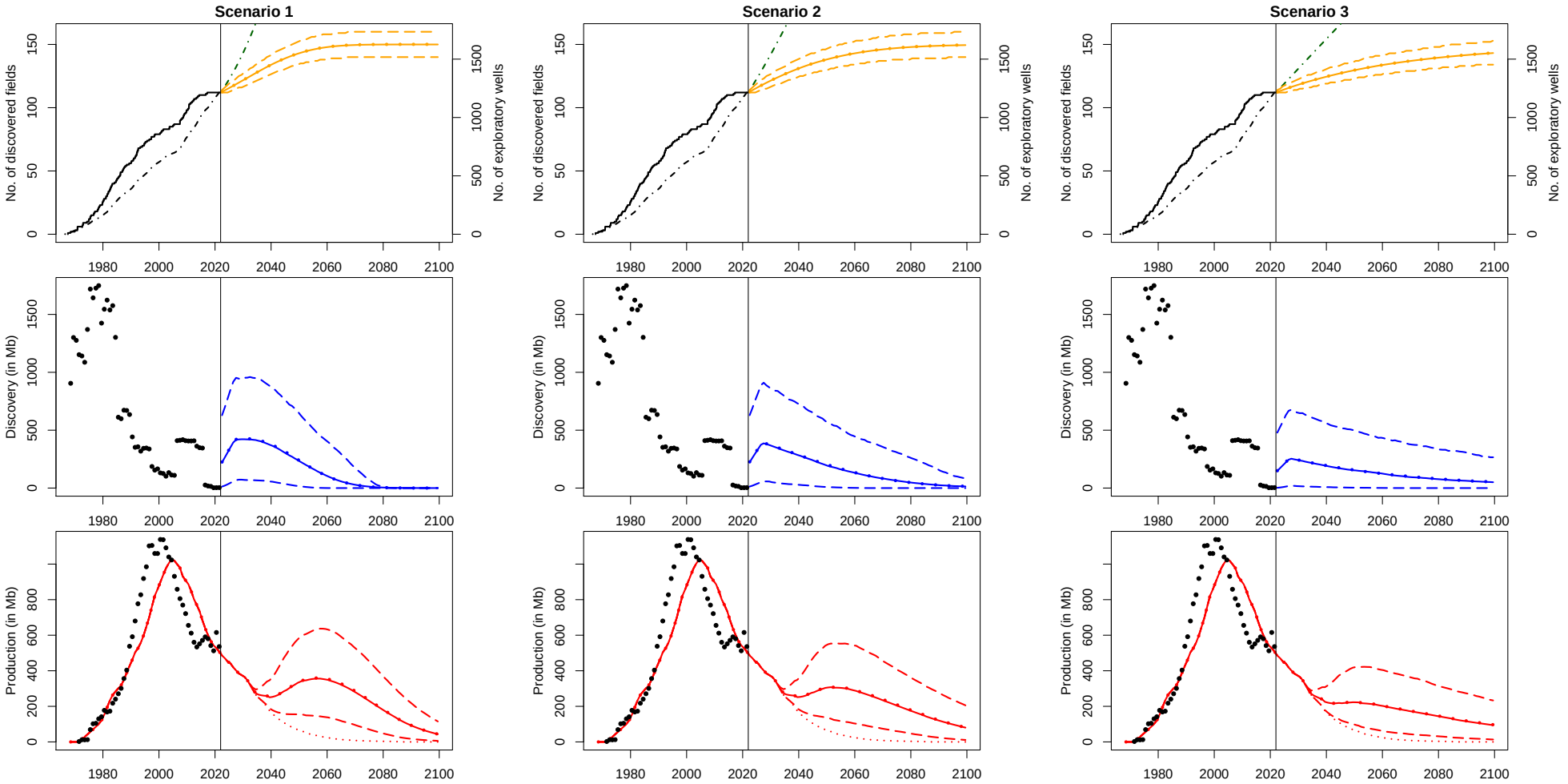

Figure B.20: Simulation results for GOM Deep ($\underline{t} = 2005$, ML-EST, assumption (4b))

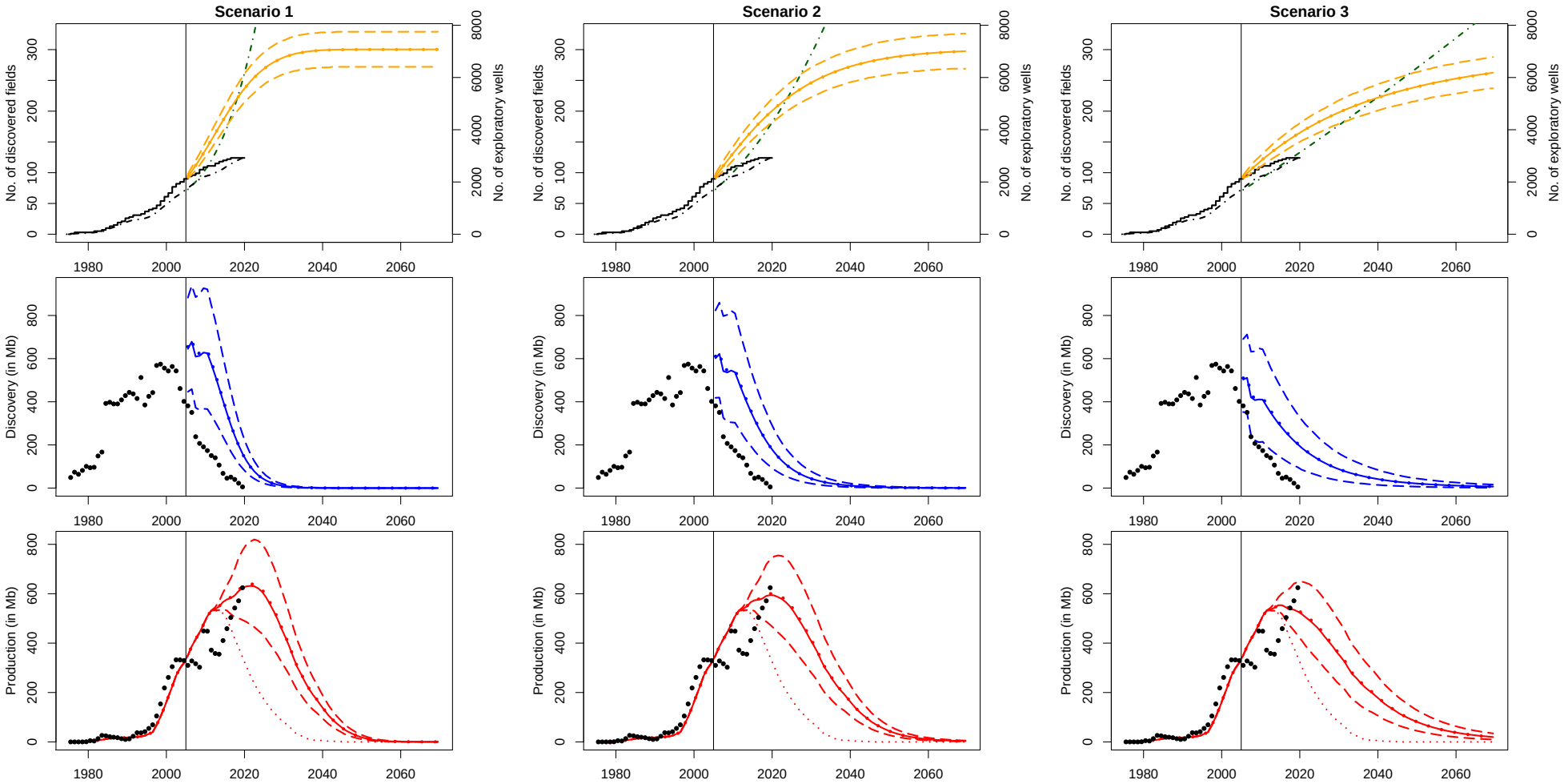

Figure B.21: Simulation results for GOM Deep ($\underline{t} = 2005$, FIT-URR, assumption (4b))

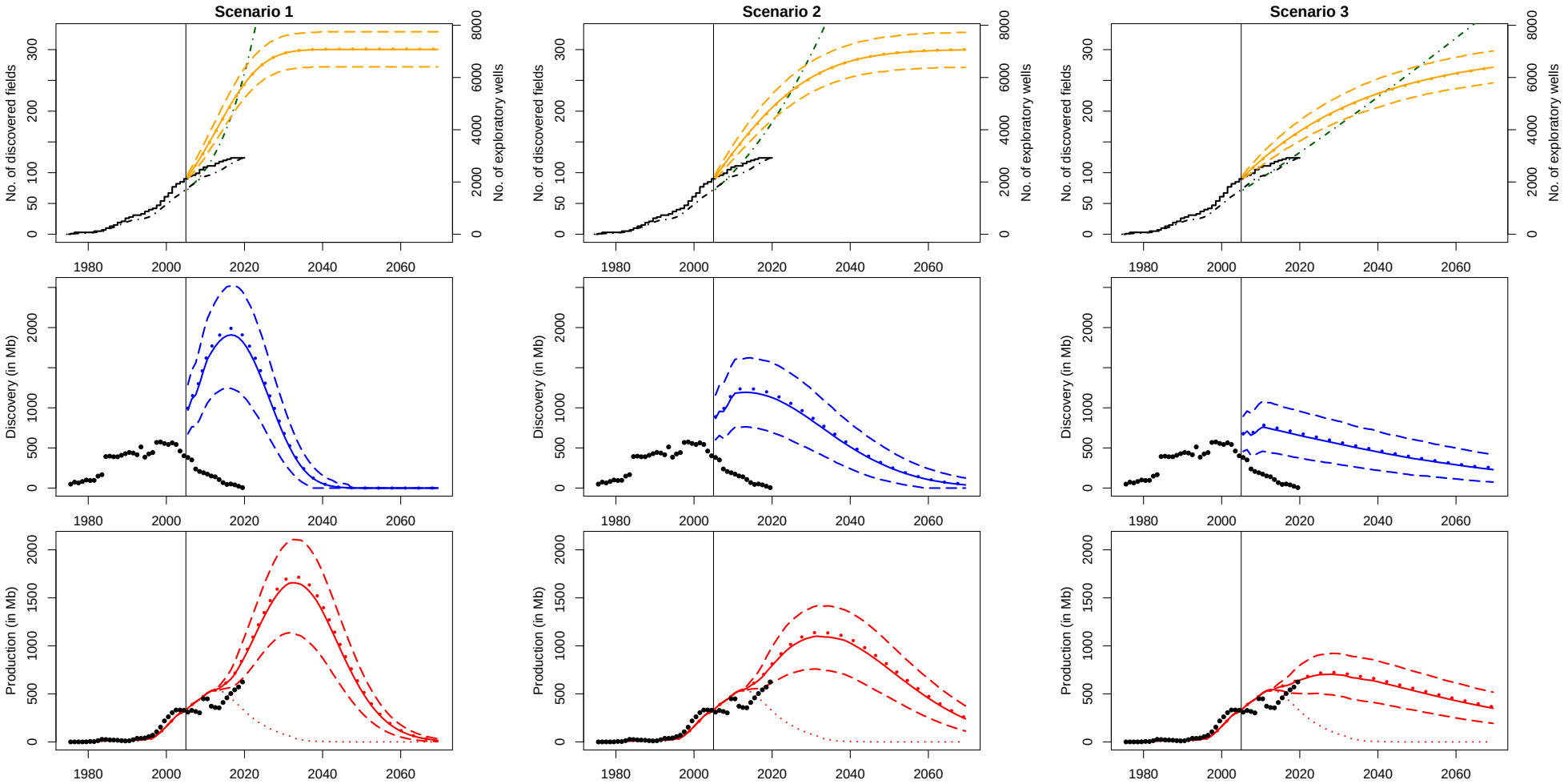

Figure B.22: Simulation results for GOM Deep ($\underline{t} = 2005$, FIT-URR, assumption (4a))

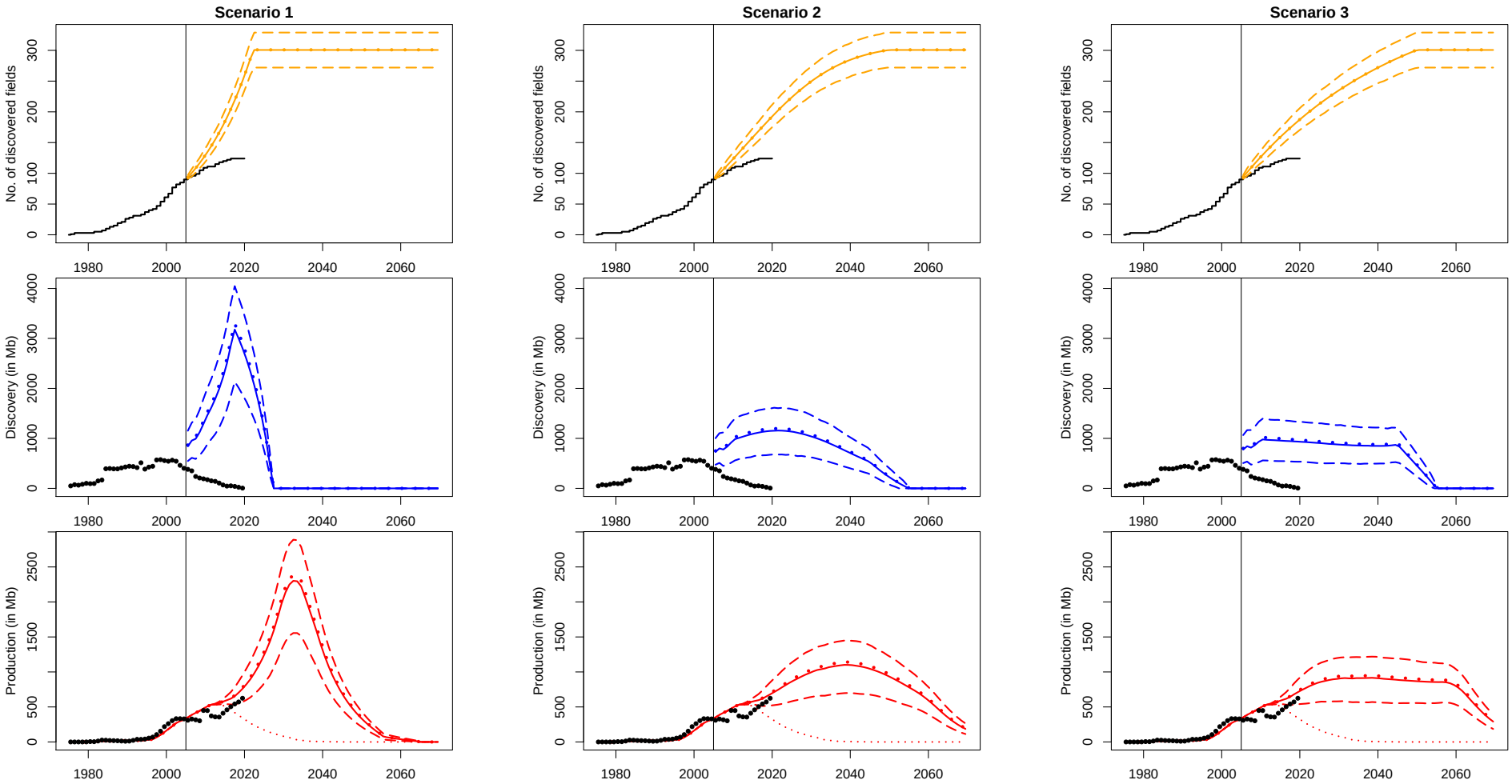

Figure B.23: Simulation results for GOM Deep ($\underline{t} = 2020$, ML-EST, assumption (4b))

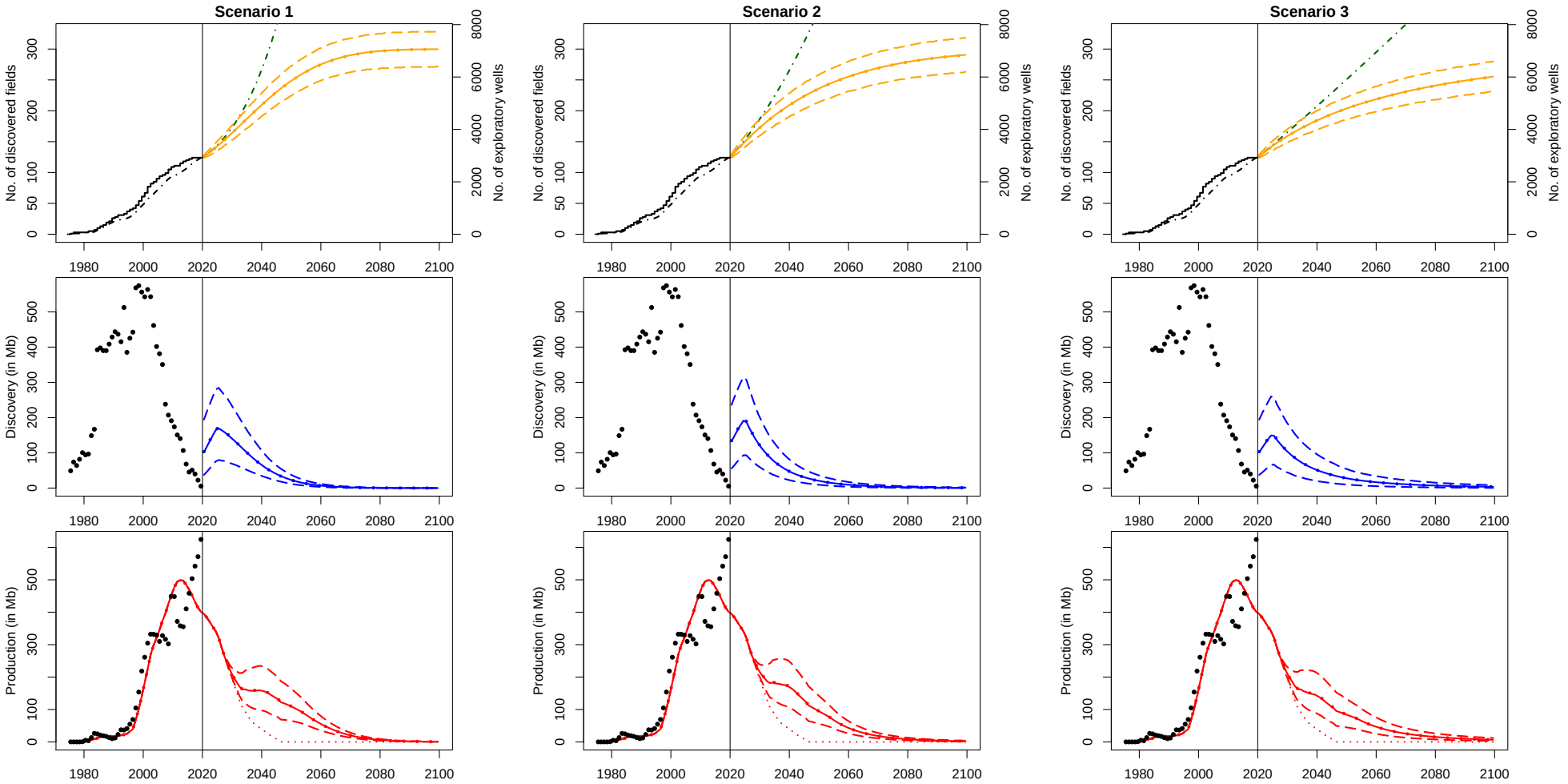

Figure B.24: Simulation results for GOM Deep ($\underline{t} = 2020$, FIT-URR, assumption (4b))